Progressive Steps towards Global Validated Simulation of Edge Plasma Turbulence

P. Ricci, A. Fasoli, I. Furno, J. Loizu, S. Jolliet, F. Halpern, A. Mosetto, B.N. Rogers[1] and C. Theiler

Ecole Polytechnique Fédérale de Lausanne (EPFL), Centre de Recherches en Physique des Plasmas, Association Euratom-Confédération Suisse, CH-1015 Lausanne, Switzerland

[1] Department of Physics and Astronomy, Dartmouth College, Hanover NH 03755

1. Introduction and Motivation

- Global 3D fluid simulations of SOL plasma turbulence are presented using the GBS code [1]
- Interplay between the plasma outflow from the core, perpendicular transport and parallel losses at the limiter
- No separation between equilibrium and fluctuating quantities

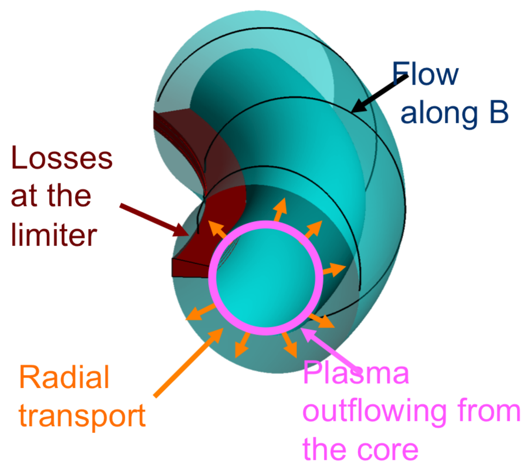

2. Progressive approach using basic plasma physics devices

- GBS has been used for simulating basic plasma physics devices of increasing complexity: linear devices (LAPD, HelCat)[2] and Simple Magnetized Toroidal plasmas (TORPEX, Helimak) [3]

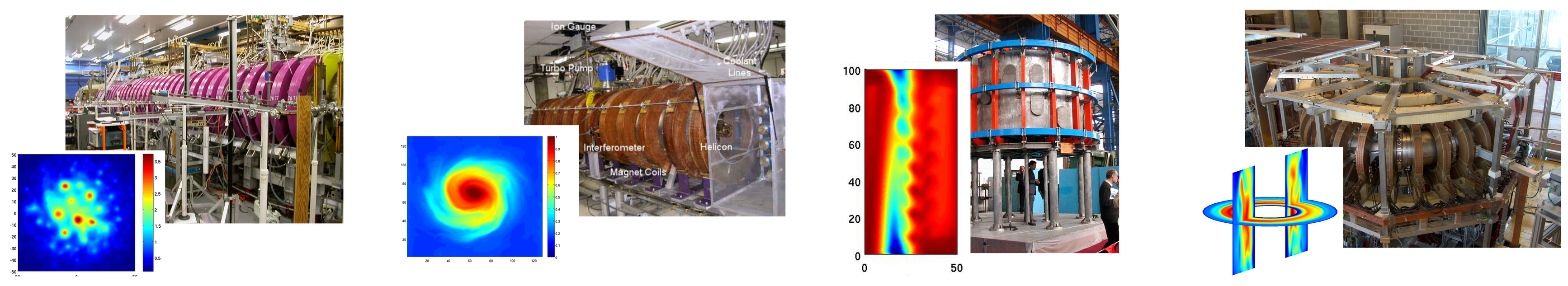

LAPD HelCat Helimak TORPEX

- Unstable linear modes, saturation mechanism, biasing effects have been analyzed
- Most of the investigations have been focused on the TORPEX device (see poster EX/P6-28)
- We are now approaching the description of the tokamak SOL, by starting from a simple setup

3. Simulation Model

- Drift-reduced Braginskii equations [4] with cold ion approximation $T_i = 0$

$$\frac{\partial n}{\partial t} = -\frac{R_0}{B}[\phi, n] + \frac{2}{B}[C(p_e) - C(\phi)] - \nabla\cdot(n V_{\parallel e}\mathbf{b}_0) + \mathcal{D}_n(n) + S_n$$

$$\frac{\partial \omega}{\partial t} = -\frac{R_0}{B}[\phi, \omega] - V_{\parallel i}\mathbf{b}_0\cdot\nabla\omega + \frac{B^2}{n}\nabla\cdot(j_\parallel \mathbf{b}_0) + \frac{2B}{n}C(p_e) + \frac{B}{3n}C(G_i) + \mathcal{D}_\omega(\omega)$$

$$\frac{\partial \chi}{\partial t} = -\frac{R_0}{B}[\phi, V_{\parallel e}] - V_{\parallel e}\mathbf{b}\cdot\nabla V_{\parallel e} + \frac{m_i}{m_e}\left(\nu\frac{j_\parallel}{n} + \mathbf{b}\cdot\nabla\phi - \frac{1}{n}\mathbf{b}\cdot\nabla p_e - 0.71\mathbf{b}\cdot\nabla T_e - \frac{2}{3n}\mathbf{b}\cdot\nabla G_e + \frac{1}{n}G_e\nabla\cdot\mathbf{b}\right) + \mathcal{D}_{V_{\parallel e}}(V_{\parallel e})$$

$$\frac{\partial V_{\parallel i}}{\partial t} = -\frac{R_0}{B}[\phi, V_{\parallel i}] - V_{\parallel i}\mathbf{b}\cdot\nabla V_{\parallel i} - \frac{1}{n}\mathbf{b}\cdot\nabla p_e - \frac{2}{3n}(\vec{b}\cdot\nabla)G_i - \frac{G_i}{n}\nabla\cdot\mathbf{b}_0 + \mathcal{D}_{V_{\parallel i}}(V_{\parallel i})$$

$$\frac{\partial T_e}{\partial t} = -\frac{R_0}{B}[\phi, T_e] - V_{\parallel e}\mathbf{b}\cdot\nabla T_e + \frac{4T_e}{3B}\left[\frac{1}{n}C(p_e) + \frac{5}{2}C(T_e) - T_e C(\phi)\right] + \frac{2T_e}{3}\left[0.71\nabla\cdot(j_\parallel\mathbf{b}_0) - \nabla\cdot(V_{\parallel e}\mathbf{b}_0)\right] + \mathcal{D}_{T_e}(T_e) + \mathcal{D}^{\parallel}_{T_e}(T_e) + S_{T_e}$$

with

$$\nabla^2_\perp\phi = \omega, \vec{\nabla}^2_\perp\delta\psi = \frac{4\pi e}{c}n(V_{\parallel i} - V_{\parallel e}), \chi = V_{\parallel e} + \frac{m_i}{m_e}\frac{\beta}{2}\delta\psi, [A, B] = \mathbf{b}\cdot(\nabla A\times\nabla B)$$

$$G_i = -3\eta_{0i}\left[\frac{2}{3}\mathbf{b}_0\cdot\nabla V_{\parallel i} - \frac{1}{3}V_{\parallel i}\nabla\cdot\mathbf{b}_0 + \frac{1}{B}\hat{C}(\phi)\right]$$

$$G_e = -3\eta_{0e}\left[\frac{2}{3}\mathbf{b}_0\cdot\nabla V_{\parallel e} - \frac{1}{3}V_{\parallel e}\nabla\cdot\mathbf{b}_0 + \frac{1}{B}\left(-\frac{1}{n}\hat{C}(p_e) + \hat{C}(\phi) + \frac{2}{3}nC(p_e) - \frac{2}{3}C(\phi)\right)\right]$$

$$\mathbf{b}\cdot\nabla A = \mathbf{b}_0\cdot\nabla A + \frac{\beta_e R_0}{2\ B}[\delta\psi, A], C(A) \equiv \frac{B}{2}\left(\nabla\times\frac{\mathbf{b}}{B}\right)\cdot\nabla A$$

- Circular concentric magnetic surfaces:

$$\vec{B}_0 = \frac{B_a R_0}{R}\vec{e}_\varphi + \frac{B_a\epsilon}{q\sqrt{1-\epsilon^2}}\vec{e}_\theta$$

- Local magnetic shear: $\partial_x \to \partial_x + (y/a)\hat{s}\partial_y$
- Limiter on the high-field side, equatorial plane
- Localized density and temperature sources around x_0

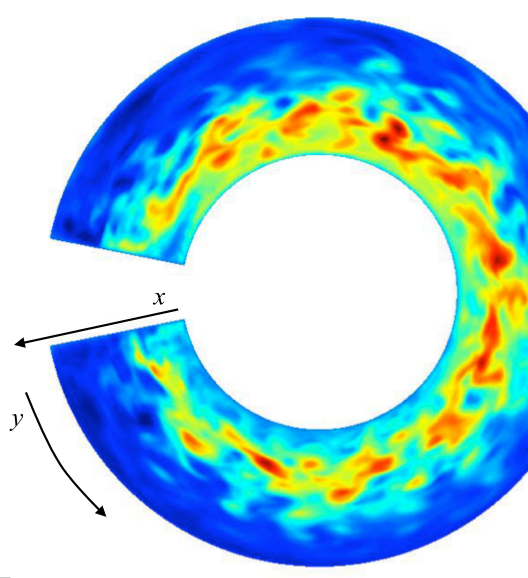

4. Boundary conditions at the magnetic presheath

- BC at the Magnetic Presheath Entrance, where Inertial Drift Approximation breaks down [5]
- Gradients normal to the wall dominate
- $\rho_e \ll \lambda_{De} \ll \rho_s \ll \lambda_{mfp} \ll L$

$$\partial_y n = -\frac{n}{c_s}\partial_y V_{\parallel i}$$

$$\partial_y \phi = -c_s\partial_y V_{\parallel i}$$

$$\omega = -\left[(\partial_y V_{\parallel i})^2 + c_s\partial^2_y V_{\parallel i}\right]$$

$$\partial_y T = \alpha\partial_y\phi, \alpha \cong 0.1$$

$$V_{\parallel e} = \sqrt{T_e}\exp(\Lambda - \phi/T_e)$$

$$V_{\parallel i} = c_s$$

- MPE BC allow a finite current at the limiter plates.
- Inconsistent BC at the limiter for n, T_e, ω lead to a polluted spectrum.
- This problem is removed by using MPE BC.

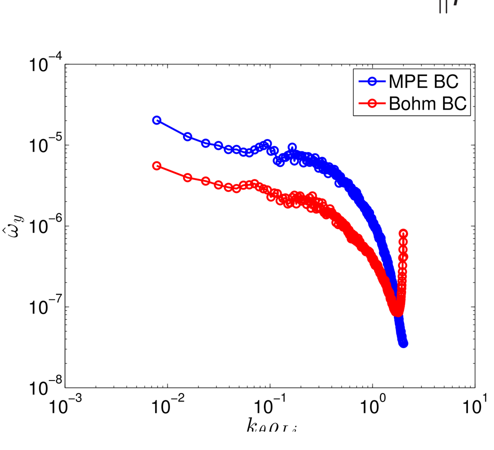

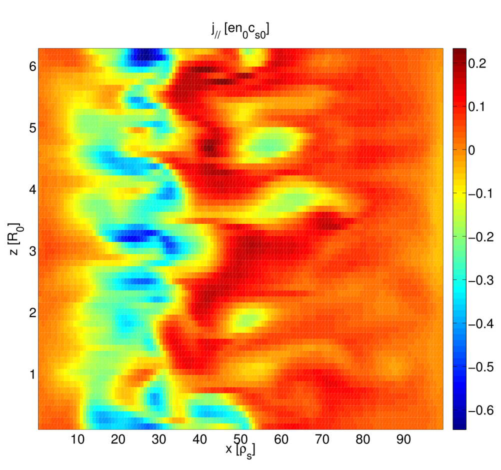

5. Numerics

- $(x, y, z) = (r, a\theta_*, R_0\varphi)$ coordinates, parallelized in x and z
- Second order centered finite difference scheme
- Arakawa scheme for the Poisson bracket operator
- Integer q constraint $\Rightarrow$ grid aligned $\mathbf{b}_0\cdot\nabla$ operator
- 4th order RK scheme for time integration
- $\phi, \delta\psi$ obtained from a linear system using one of LAPACK, Pardiso, MUMPS
- Typical resolution: $N_x = 128, N_y = 512, N_z = 64, \Delta t = 2\cdot10^{-4}R/c_s$, $\sim 2\cdot10^5$ CPUh on HELIOS

6. Linear theory

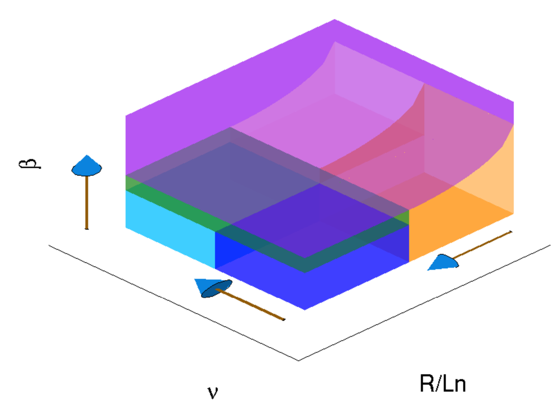

Regions of existence of the instabilities as a function of ν, R/L_n and β [6]:

- Resistive Ballooning
- Inertial Ballooning
- Ideal Ballooning
- Resistive Drift Wave
- Inertial Drift Wave
- region of suppression of the Drift Wave

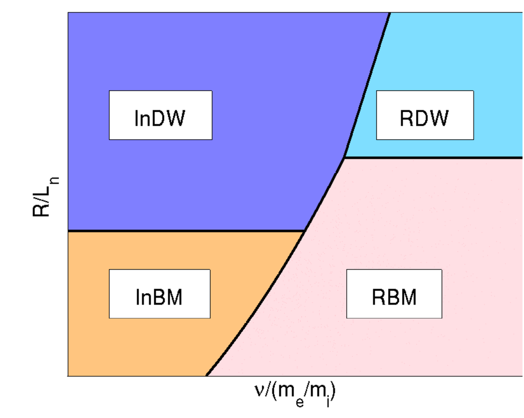

7. Nonlinear simulations

A) Saturation mechanism

- Turbulence can saturate because: (a) it removes its drive (b) Kelvin-Helmholtz saturate its growth
- Gradient-removal mechanism: $\partial p_{e1}/\partial r \sim \partial p_{e0}/\partial r \to p_{e1} \sim p_{e0}/(L_p k_r)$ Estimating $\phi_1 \sim \gamma L_p p_{e1}/(k_y p_{e0})$ and $k_r \sim \sqrt{k_y/L_p}$ the radial flux is : $\Gamma_r = \left\langle p_{e1}\frac{\partial\phi}{\partial y}\right\rangle \sim \frac{p_{e0}}{L_p}\frac{\gamma}{k_r^2} \sim \frac{\gamma p_{e0}}{k_y}$
- KH gives $\phi_1 \sim \gamma/(k_y k_r)$, $k_r \sim k_y$, $\Gamma_r \sim \frac{\gamma p_{e0}}{L_p k_y^2}$
- $\Gamma_r^{KH}/\Gamma_r^{GR} \sim 1/(k_y L_p) < 1$, but KH stable if $\sqrt{k_y L_p} > 3$
- In steady state, balancing perpendicular transport and parallel losses $\partial\Gamma_r/\partial r \sim \Gamma_r/L_p \sim (p_0 c_s)/(qR)$, which gives $L_p \sim Rq\gamma/(k_y c_s)$ in GR-saturated simulations

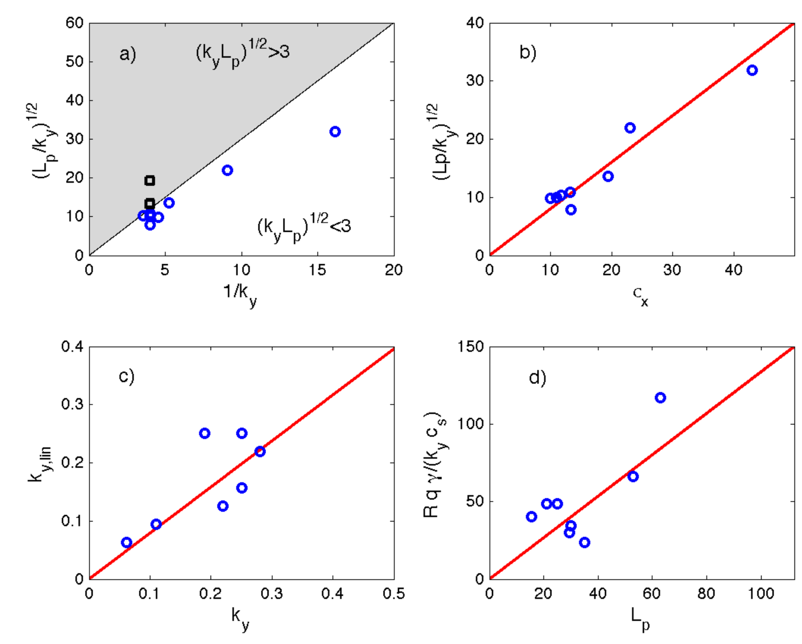

B) Simulations with magnetic shear

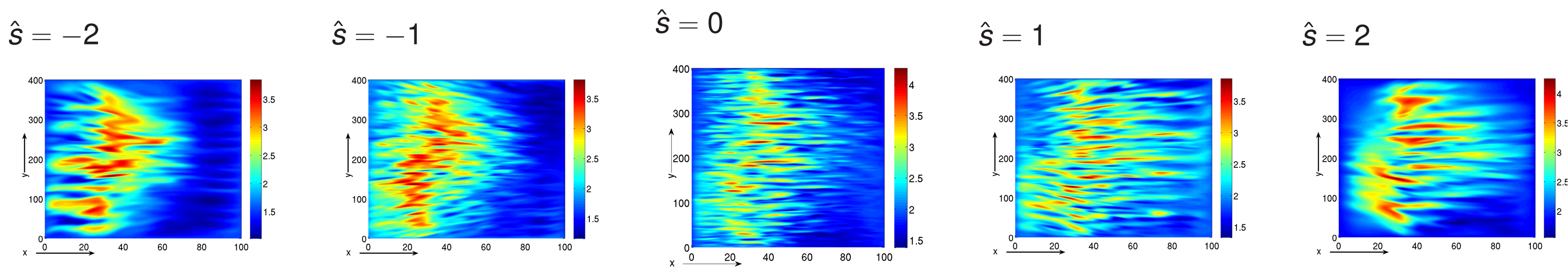

$\hat{s} = -2$	$\hat{s} = -1$	$\hat{s} = 0$	$\hat{s} = 1$	$\hat{s} = 2$
$L_n = 26.19$, $L_t = 42.52$, $L_p = 16.21$	$L_n = 37.45$, $L_t = 51.29$, $L_p = 21.65$	$L_n = 61.44$, $L_t = 77.06$, $L_p = 34.05$	$L_n = 62.43$, $L_t = 83.10$, $L_p = 35.65$	$L_n = 50.58$, $L_t = 73.69$, $L_p = 30.00$

Reduction of L_p for both positive and negative values of the shear, with respect to the shearless case with almost constant Γ_x => damping of the instability

C) EM simulations

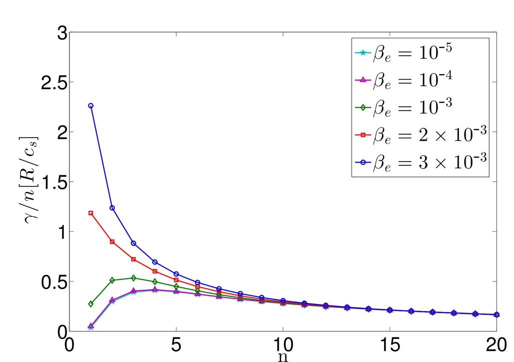

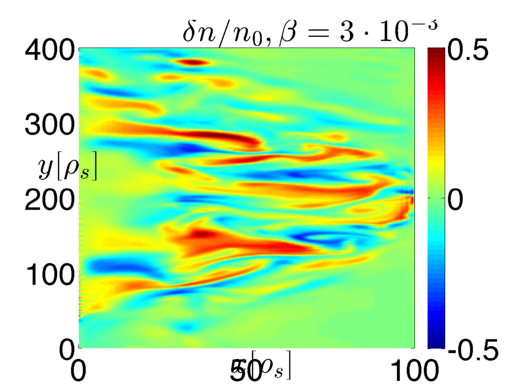

- Transition from Resistive to Ideal Ballooning modes
- Saturation mechanism $\Rightarrow$ transport dominated by max(γ/n)
- In EM NL simulations, a global mode $n = 1$ becomes dominant

8. Validation Methodology and application to TORPEX

- Identification of the observables to use for the validaton
- Classification of the observables into a primacy hierarchy: the lower the level in the hierarchy, h_j, the more stringent the comparison. Examples: 0^{th} level: I_{sat}^{exp}, n^{sim}; 1^{st} level: n^{exp}...
- Definition of the agreement for each observables, R_j
- Global metric: $\chi = \sum_j R_j H_j S_j / (\sum_j H_j S_j)$, with $H_j = 1/(1 + h_j^{exp} + h_j^{sim})$, $S_j = \exp[-(\Delta obs^{sim} + \Delta obs^{exp})/(|obs^{sim}| + |obs^{exp}|)]$.
- The methodology has been tested on the TORPEX devices, using 11 observables: $n(r)$, $T_e(r)$, $\phi(r)$, skewness(r), kurtosis(r), $\tilde{n}$, I_{sat}, fluctuations pdf, psd, k_z, spectrum, k_φ
- The results of a 2D and 3D GBS simulations have been validated [7]

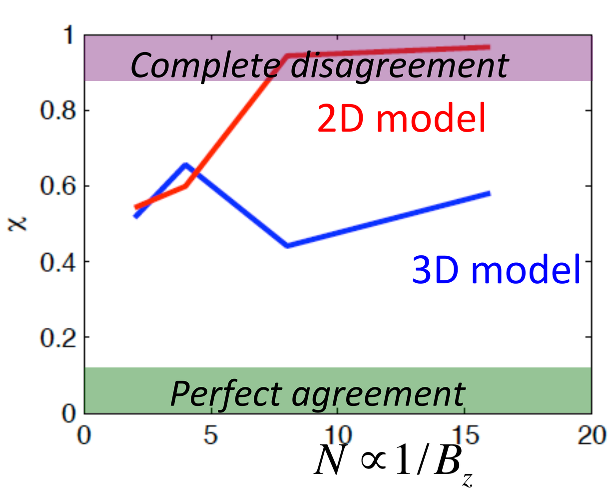

9. Conclusions

- By using a progressive approach, GBS is now capable of evolving plasma turbulence in limited SOL
- Self-consistent boundary conditions at the limiter plates
- Identification of the linear instability phase space, turbulence saturation mechanisms, the role of magnetic shear, and electromagnetic effects

References :
[1] P. Ricci et al., submitted to Plasma Phys. Contr. Fusion
[2] B. N. Rogers and P. Ricci, Phys. Rev. Lett. 104, 225002 (2010)
[3] P. Ricci and B. N. Rogers, Phys. Rev. Lett. 104, 145001 (2010)
[4] A. Zeiler et al., Phys. Plasmas 4, 2134 (1997)
[5] J. Loizu et al., Phys. Rev. E 83, 016406 (2011); J. Loizu et al., submitted to Phys. Plasmas
[6] A. Mosetto et al., accepted on Phys. Plasmas
[7] P. Ricci et al. Phys. Plasmas 16, 055703 (2009); P. Ricci et al. Phys. Plasmas 18, 032109 (2011)